Environmental Science
Water Research & Technology

ROYAL SOCIETY OF CHEMISTRY

PAPER

View Article Online
View Journal | View Issue

Cite this: *Environ. Sci.: Water Res. Technol.*, 2026, **12**, 684

Fate and transformation of quinone outside inhibitor (QoI) fungicides during simulated drinking water treatment processes

Christopher J. Knutson,†[abc] Abigail M. Carlin,†[a] Sania Kamran,[b] James B. Gloer [a] and David M. Cwiertny *[abcd]

Quinone outside inhibitor fungicides (QoIs) are widely used across the United States, with common QoIs (*e.g.*, azoxystrobin, pyraclostrobin) regularly detected in water resources that could serve as drinking water supplies in agriculturally dominated watersheds. Here, we explored the fate of several QoIs during simulated water treatment *via* coagulation/flocculation, chemical (lime-soda) softening, chemical disinfection with free chlorine, and granular activated carbon (GAC). Jar tests with Iowa River water found little QoI removal during coagulation/flocculation. Trifloxystrobin and kresoxim-methyl underwent base-promoted hydrolysis at pH values and over timescales used in lime-soda softening, with liquid chromatography-tandem mass spectrometry (LC-MS/MS) and nuclear magnetic resonance (NMR) data identifying known acid metabolites as major hydrolysis products. Select QoIs, kresoxim-methyl, pyraclostrobin, azoxystrobin, fenamidone, and dimoxystrobin, were reactive toward free chlorine under conditions and over timescales relevant for chemical disinfection, resulting in persistent, often chlorinated, transformation products. Notably, we observed distinct reaction sites during chlorination for each of the five QoIs found to be reactive toward free chlorine, including some cases where the biologically active moiety of the parent molecule was conserved. Successful management of QoIs can likely be achieved with GAC, which quickly removed all QoIs *via* sorption. Outcomes of this work will help to improve exposure assessments to QoIs and their transformation products through drinking water, while also identifying practical approaches for their removal during drinking water treatment.

Received 13th October 2025,
Accepted 18th December 2025

DOI: 10.1039/d5ew01004g

rsc.li/es-water

Water impact

Widely used quinone outside inhibitor (QoI) fungicides can enter drinking water sources *via* runoff, yet their fate during water treatment is poorly understood. Laboratory studies found some QoIs persist through conventional treatment, while others transformed during softening and chemical disinfection into potentially bioactive products. Advanced treatment with activated carbon effectively removed all tested QoIs. These findings will help water systems in agricultural regions manage QoIs and reduce consumer exposure risks.

Introduction

Fungal pathogens are a leading cause of crop loss, resulting in the application of fungicides to prevent pathogen growth and increase crop yields.[1,2] Quinone outside inhibitors (QoIs) are a major class of fungicides that inhibit energy production in fungi by binding to the quinol oxidation site and blocking electron transfer between cytochrome b and cytochrome c1.[3] Due to their effectiveness, QoIs have become one of the most widely used classes of fungicides with worldwide sales growing from $620 million USD in 1999 (ref. 4) to $3.8 billion USD in 2016.[5]

In 2016 alone, 2.5 million pounds of azoxystrobin, among the most popular of QoIs, were applied to crops, representing a 250% increase from 2006.[6] Notably, these estimates from the United States Geological Survey's (USGS) Pesticide National Synthesis Project are likely low, as many QoIs fungicides are applied as seed treatments, which have not been accurately accounted for in USGS pesticide use data since 2015.

[a] *Department of Chemistry, University of Iowa, Iowa City, IA 52242, USA*
[b] *Department of Civil & Environmental Engineering, University of Iowa, 4105 Seamans Center, Iowa City, IA 52242, USA. E-mail: david-cwiertny@uiowa.edu; Tel: +(319) 335 1401*
[c] *IIHR-Hydroscience & Engineering, University of Iowa, Iowa City, IA 52242, USA*
[d] *Center for Health Effects of Environmental Contamination, University of Iowa, Iowa City, IA 52242, USA*
† Equal contribution as lead author for CJK and AMC.

Despite their extensive use, relatively little is known about the fate of QoI fungicides in the environment. Estimated octanol–water partitioning coefficients ($\log K_{ow}$ values) for QoIs range from 2.8 to 4.5, suggesting moderate hydrophobicity and the potential for some environmental mobility (Table S1).[7] QoIs have been detected in surface water, groundwater, and sediment worldwide.[8–11] For example, azoxystrobin was detected in 12 out of 18 German streams in lowland agricultural areas, with dissolved concentrations ranging up to 29.7 μg L^{-1}.[10] Likewise, in the United States azoxystrobin was detected in 45 out of 103 water samples collected from 29 agriculturally impacted streams, with a maximum concentration of 1.13 μg L^{-1}.[11] Pyraclostrobin, another popular QoI, has also been detected in the United States in groundwater (30% of 12 groundwater samples with a maximum concentration of 3.1 ng L^{-1})[9] and sediment within streams draining agricultural areas (75% of 32 samples with a maximum loading of 198 μg kg^{-1}).[8] Recent monitoring data of rivers and streams in Minnesota detected azoxystrobin in 19% of samples (out of 289 tested), with a maximum concentration of 729 ng L^{-1}.[12]

Because fungicides are applied to crops as much as 10 times throughout the growing season,[9] it is probable that non-target organisms, including humans, experience some level of chronic exposure to these chemicals. Furthermore, there is emerging evidence that, as a class, QoI fungicides may pose threats to ecosystem and human health. A recent investigation found that pyraclostrobin, trifloxystrobin, famoxadone, and fenamidone can stimulate the production of free radicals, which disrupt microtubules in neurons, potentially contributing to neurodegenerative diseases such as Alzheimer's disease, Huntington's disease, and autism.[13] In another study, short term exposure (24–72 h) to 100 ng L^{-1} (ref. 14) of azoxystrobin was found to have adverse effects on fish. Larval stages were most susceptible, and the reported oxidative damage caused cell death after 48 h. The authors proposed that azoxystrobin might affect mitochondrial respiration in zebrafish larvae, which is important for generation of energy for growth and reproduction, while effects on immune and reproductive genes and hormone levels (estradiol) were also noted at this exposure level. Notably, this level of exposure is less than what has been observed for azoxystrobin in surface waters, and well below the chronic toxicity value for invertebrates developed by EPA (44 000 ng L^{-1}).[15]

Given their prevalence in agriculturally impacted surface waters, it is plausible that QoIs will be present in drinking water sources in areas of intense agricultural production. Although available $\log K_{ow}$ values suggest they may be prone to removal *via* granular or powdered activated carbon treatment (see Table S1),[7] many small- to medium-sized water treatment plants in areas like the U.S. Midwest do not rely on activated carbon due to associated cost and waste disposal, nor has this result been previously verified experimentally. Moreover, considering their structures, transformation during certain water treatment processes is possible. For example, during chemical softening, the ester moieties on some QoIs (*e.g.*, trifloxystrobin and kresoxim-methyl) have the potential to undergo base-mediated hydrolysis,[16] as we have recently observed with the neonicotinoid thiamethoxam and the dichloroacetamide safener benoxacor.[13,17,18] Likewise, because QoIs contain at least one aromatic ring, they may undergo electrophilic substitution in the presence of chemical oxidants such as chlorine.[19] Indeed, azoxystrobin residues on table grapes were reduced by 50% and 90% *via* fumigation with ClO_2 and O_3, respectively.[19,20] However, corresponding analysis and identification of potential transformation products was not performed under these conditions.

Here, to fill existing gaps regarding the persistence and transformation of QoIs in the environment, we experimentally evaluated the fate of several common QoI fungicides during simulated water treatment processes including coagulation/flocculation/sedimentation, chemical softening, sorption on activated carbon, and chemical disinfection with free chlorine. Although all QoIs appear amenable to removal by activated carbon, we find that some, but not all, QoIs can be readily transformed under the alkaline and oxidizing conditions of chemical softening and disinfection, respectively. Accordingly, we conducted base-mediated hydrolysis experiments in both idealized (*i.e.*, buffered solutions) and real (*i.e.*, water from the chemical softening basin of a water treatment plant) aqueous systems using conditions and timescales relevant to chemical softening, while also exploring QoI chlorination under conditions representative of water treatment and distribution. To assist with QoI fate modeling, we report kinetic rate constants for base-mediated hydrolysis and chlorination under simulated water treatment, while also using liquid chromatography-tandem mass spectrometry (LC-MS/MS) and nuclear magnetic resonance (NMR) data to identify the major transformation products generated from these chemical treatment processes. Outcomes of this work will help to better quantify the extent of QoI removal during drinking water treatment and their potential to yield bioactive transformation products, in turn improving assessments of their associated human health risks through drinking water exposure.

Materials and methods

Reagents

PESTANAL® analytical standards (96–99% purity) for azoxystrobin (AZX), dimoxystrobin (DMX), fenamidone (FNM), fenamidone metabolite RPA 410193, fluoxastrobin (FLU), kresoxim-methyl (KM), picoxystrobin (PIC), pyraclostrobin (PYR), trifloxystrobin (TRI), and trifloxystrobin free acid (also known as trifloxystrobin metabolite CGA 321113) were obtained from Sigma-Aldrich. A complete reagents list is provided in the SI.

QoI stock solution preparation

For most experiments, stock solutions (10 mM) of each QoI were prepared in acetonitrile (ACN) and contained in amber glass vials to prevent incidental light exposure. QoIs were dosed into experimental systems to achieve concentrations between 0.31–6.2 mg L^{-1} (a range below reported solubilities; see Table S1). This approach resulted in volumes corresponding to less

than 0.25% (v/v) ACN in the experimental system to minimize carrier solvent effects.[21] For QoI sorption on GAC, experiments were conducted in saturated aqueous solutions of each QoI prepared in appropriate aqueous buffer.

Coagulation and flocculation experiments

Coagulation and flocculation experiments were conducted using a standard jar test apparatus following the experimental procedures in Hladik *et al.*[22] Experiments were conducted with each QoI individually. Coagulant iron(III) chloride ($FeCl_3$) was dosed to a final concentration of 40 mg L^{-1} from a 1.5% w/w aqueous solution into 0.5 L of raw water from the Iowa River that had been spiked with 1 μM of each QoI. This coagulant dose was chosen as sufficient to remove more than 40% of the total organic carbon (TOC) initially present in the water sample, as approximated from the decrease in UV absorbance measurements at 254 nm. River water samples were obtained from the University of Iowa's Water Treatment Plant (UI WTP), which uses the Iowa River as source water, in January 2020. Typical TOC levels in the Iowa River in January range from 3.5–4.0 mg L^{-1}.

Using a Phipps & Bird PB-700 Jartester, solutions were initially mixed at 100 RPM for 2 min, mixed at 20 RPM for 1 h, and then allowed to settle with no mixing for 1 h. Aqueous samples were then withdrawn from the supernatant using a glass pipette, transferred to 2 mL amber HPLC vials, and analyzed within 24 h of sample collection. Control experiments were conducted using 0.22 μm filtered Iowa River water to which no coagulant was added. The percent removal of QoIs during coagulation and flocculation was reported by comparing removal in systems treated with coagulant to concentrations measured in control systems.

Chemical softening experiments

To simulate the alkaline conditions used during chemical softening, we prepared 10 mM sodium carbonate solutions (1000 mg L^{-1} as $CaCO_3$) ranging from pH 10 to 10.8. This pH range is typical of that used for chemical softening with lime at the UI WTP.[17] We also conducted these experiments in water samples collected from the effluent of the chemical softening basin at the UI WTP, which were passed through 0.22 μm filters prior to use.

To initiate experiments, QoIs were dosed into buffer solutions *via* a glass syringe from 10 mM stock solutions in ACN. After dosing the reactors with QoIs, the solution was rapidly mixed, and a sample was collected immediately for analysis *via* HPLC with diode array detector (DAD) to estimate the initial concentration in the reactor. By automating the HPLC injection, sequential sampling from the same vial was conducted such that each injection occurred at regular 20-minute intervals. Although most experiments were conducted at ambient laboratory temperature (~20–22 °C), we also examined seasonal temperature dependence for select QoIs by determining rate constants for hydrolysis at low (5 °C) and high temperature (35 °C). For these experiments, samples were housed in a water bath to maintain a constant temperature and analyzed immediately after collection. For structural identification of major transformation products generated *via* chemical softening, experimental conditions were scaled up to facilitate product isolation and analysis as described in the SI.

Chlorination experiments

To initially assess QoI reactivity toward free chlorine and determine reaction rate constants, chlorination experiments were carried out with QoI concentrations higher than environmentally relevant. First, QoIs were dosed into 40 mL amber glass reaction vessels containing 20 mL sodium phosphate buffer (pH 7, 5–10 mM; additional experiments revealed the buffer concentration did not influence rates of QoI transformation, see Fig. S1) and mixed vigorously by hand. After mixing, 0.5 mL of the solution was collected for analysis to estimate the initial QoI concentration in the reactor. Chlorination reactions were initiated by dosing with an aqueous HOCl stock solution to produce final chlorine concentrations ranging from 5.6–62 mg L^{-1} as Cl_2. At least a 10-fold (up to 320-fold) excess concentration of free chlorine was used to achieve pseudo-first-order decay of the QoI (*i.e.*, assuming constant chlorine concentration over time) from which second-order reaction rate constants could be determined. After the addition of the chlorine stock solution, reactions were continuously monitored *via* HPLC-DAD injection from a single 2 mL amber autosampler vial with periodic, automated injections. All chlorination experiments were performed at ambient laboratory temperatures (22–25 °C).

Product characterization experiments were conducted at two different concentration scales using an approach that considered both environmentally relevant concentrations and conditions to generate sufficient product mass for structure elucidation *via* NMR. At the environmentally relevant scale, the QoI concentration was kept at 100 μg L^{-1} and reacted with 5 mg Cl_2 L^{-1}. The other scale focused on generating enough product material for NMR analysis, requiring that we raised the starting QoI concentration to 0.25–3.0 mM. For these experiments, free chlorine was repeatedly dosed into the reaction vessel at an initial concentration of 5 mg Cl_2 L^{-1} every 4 h until a 1 : 1 molar equivalence of free chlorine (based on [HOCl]) to QoI was achieved. The reactions conducted at environmentally relevant concentrations were subject to LC-HRMS, while the products of the larger scale reactions were also interrogated by NMR analysis. Herein, we report structure elucidation *via* NMR only for products that were observed under environmentally relevant concentrations, using LC retention time matching and HRMS data to confirm their formation under scaled-up conditions necessary for product isolation. In certain instances, we observed additional products using the scaled-up reaction conditions, but we deemed these byproducts of the elevated concentrations necessary for product isolation and, thus, not likely environmentally relevant. Additional details on product isolation and characterization are detailed in the SI.

Activated carbon experiments

Uptake experiments onto GAC were conducted with saturated aqueous solutions of each QoI (0.5–8 mg L^{-1}; see Table S1) at pH 7 (5 mM phosphate buffer) to avoid the use of an organic carrier solvent that could interfere with sorption. GAC was added to the saturated solutions at a solid loading of either 0.5 or 1 g L^{-1}. Reactors were then mixed on an end-over-end rotator at 40 RPM, and samples were taken at regular intervals for analysis.

Analytical methods

The free chlorine concentration of concentrated HOCl stock solutions was determined *via* UV-visible spectroscopy using characteristic λ_{max} values for HOCl and its anionic form, OCl^- (235 at pH < 5 and 292 nm at pH > 10, respectively)[23] after dilution (0.25 mL/10 mL water) and analysis at the respective pH values. Additionally, HOCl concentration was confirmed by titration of a diluted aqueous solution of HOCl (up to 1 : 1000 NaOCl : H_2O) with ferrous ammonium sulfate [FAS, $Fe(NH_4)_2(SO_4)_2$] and DPD (*N*,*N*-diethyl-*p*-phenylenediamine).[24] All experimental aqueous samples of QoIs were analyzed within 24 h of collection using HPLC-DAD (Agilent 1260), with additional details provided in the SI.

Isolation of QoI reaction products was conducted using an Agilent 1200 series HPLC-DAD system while monitoring at 207 nm. An Apollo C_{18} semi-preparative (10 × 250 mm, 5 μm) column was used for isolation. A gradient elution method was used beginning with 50% ACN in H_2O and changing to 90% ACN over 20 minutes then returning to 50% ACN over 10 minutes for a total run length of 30 minutes at a flow rate of 2 mL min^{-1}. Additional details of instrumentation and methods for HPLC, LC-MS and NMR are provided in the SI.

Results and discussion

QoI fate during coagulation and flocculation

Results from coagulation and flocculation studies with QoIs in Iowa River water are shown in Fig. S2, which presents the percent of QoIs remaining in solution (as an average of at least duplicate experiments) after coagulation, flocculation and sedimentation. For all QoIs investigated (initially present at 1 μM), at most 10% of the initial mass (for azoxystrobin) was removed through partitioning into settling flocs. Thus, we do not anticipate that coagulation, flocculation, and sedimentation will represent a significant removal pathway for QoIs during water treatment. We note that TOC in Iowa River can range up to nearly 6 mg L^{-1} seasonally,[25] thus a greater degree of QoI removal may be observed in more organic-rich waters *via* hydrophobic interactions between the QoIs and the organic matter present in settling flocs.

QoI fate during chemical softening

Only trifloxystrobin and kresoxim-methyl were found to be reactive under alkaline conditions, each nearly entirely decomposing over 3 h in water taken from the chemical softening basin at the UI WTP (Fig. 1a). All other QoIs were stable, suggesting limited potential for their transformation over the typical timescales (1–3 h) in a conventional softening basin.[17] Moreover, and as expected for a base-mediated process, the transformation rate for trifloxystrobin and kresoxim-methyl increased with increasing pH in model (buffered) aquatic systems (*i.e.*, increasing OH^- concentration; Fig. 1b). Values for the experimentally measured pseudo-first-order rate constant (k_{obs} value) increased linearly with hydroxide concentration, producing half-lives as low as ~0.25 h at the highest pH value considered (pH ~10.8). Accordingly, second-order rate constants for the reaction of trifloxystrobin and kresoxim-methyl with hydroxide (k_{OH} in M^{-1} s^{-1}) could be determined from the slope of the best-fit linear regression in Fig. 1b, producing values of 1.08 (±0.09) and 1.12 (±0.04) M^{-1} s^{-1}, respectively. As expected, the rates of hydrolysis for kresoxim-methyl and trifloxystrobin varied with temperature, with decreasing temperatures slowing hydrolysis rates, and increasing temperatures increasing rates (Fig. S3). Values of k_{obs} at 35 °C were more than 10- and 20-fold greater than those measured at 5 °C for trifloxystrobin and kresoxim-methyl, respectively (Table S2), corresponding to half-lives on the order of 10 minutes at 35 °C.

Our analysis revealed that trifloxystrobin and kresoxim-methyl each reacted with hydroxide to yield a single transformation product (see HPLC-DAD traces in Fig. 1c and d). In each case, the products were more polar than their parent QoI, eluting several minutes earlier on a reverse-phase C_{18} HPLC column. Experiments conducted at a higher total QoI mass to facilitate product isolation yielded these same product species based on retention time matching, facilitating their NMR analysis (see Fig. S4–S9 and Tables S3 and S4, which include full ^1H NMR spectra for products of trifloxystrobin and kresoxim-methyl).

For trifloxystrobin, the ^1H NMR spectrum (Fig. S6) indicated a single change in the product relative to the starting material (Fig. S5) with the absence of a signal at δ 3.73 corresponding to the loss of a methyl unit from the methyl ester functional group to afford a free carboxylic acid moiety. Indeed, the product spectrum matched that of the trifloxystrobin free acid standard. For kresoxim-methyl, the ^1H NMR spectrum (Fig. S8) also indicated a single change in the product with the absence of a signal at δ 3.72 corresponding to the loss of a methyl unit from the methyl ester functional group to afford a free carboxylic acid moiety. This change was analogous to that observed for the trifloxystrobin product, and thus it was concluded that the product of the reaction was the kresoxim-methyl free acid. We note that the comparable reaction center and structural change for the hydrolysis of trifloxystrobin and kresoxim-methyl is consistent with the comparable values of k_{OH} that we measured for each of these species.

The base-promoted hydrolysis products identified by ^1H NMR analysis are previously known metabolites of each parent material (Fig. 1e) generated *via* ester hydrolysis. The

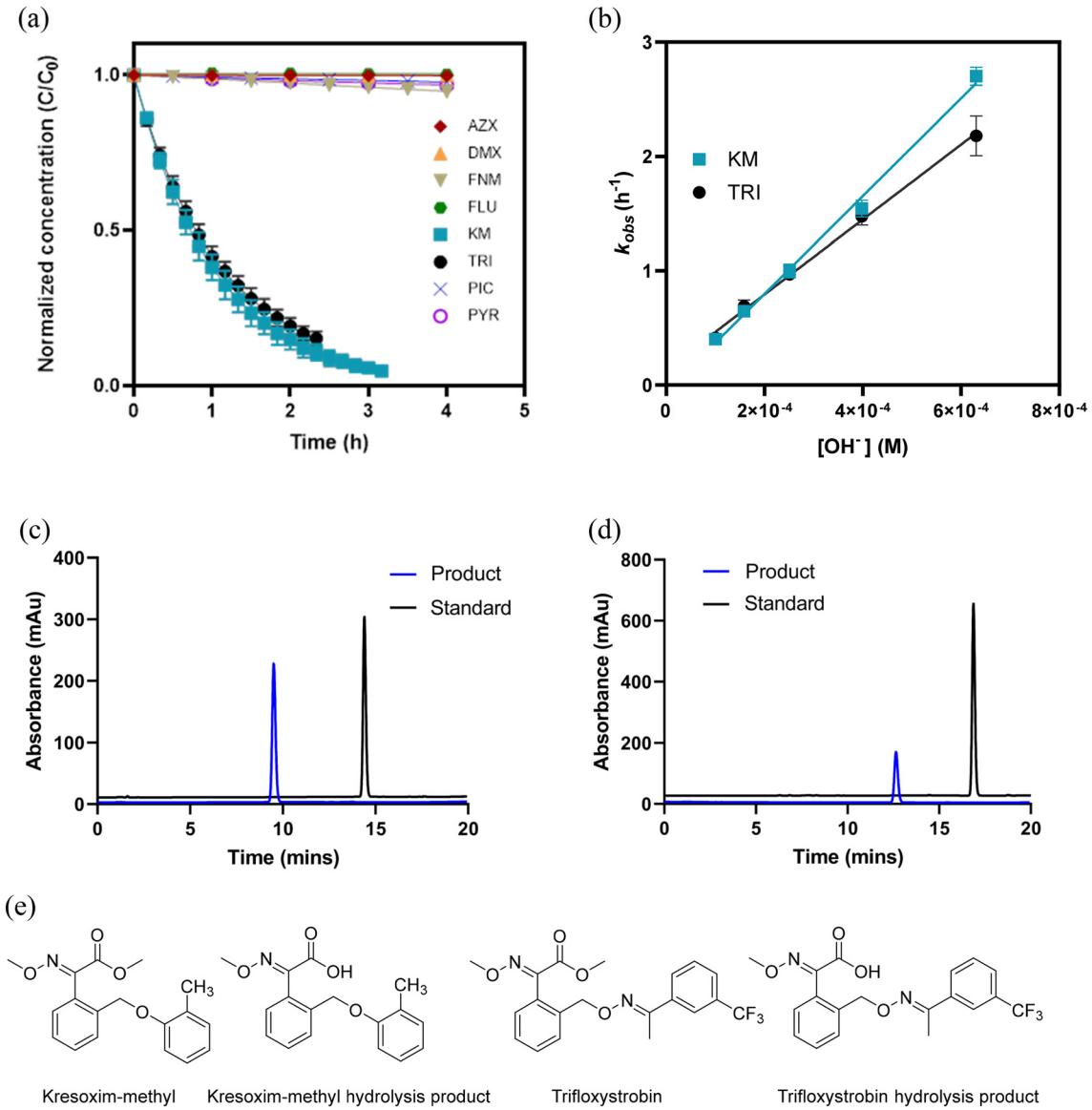

Fig. 1 (a) Normalized concentration of QoIs in water from the chemical softening basin at UI WTP (pH 10.47 ± 0.05) *versus* time and (b) values of k_{obs} *versus* [OH^-] for kresoxim-methyl and trifloxystrobin including 95% confidence intervals from linear regression analysis used to determine k_{obs} values. HPLC chromatograms depicting retention times while monitoring at 210 nm for (c) kresoxim-methyl and the kresoxim-methyl hydrolysis product and (d) trifloxystrobin and the trifloxystrobin hydrolysis product. (e) Structures of kresoxim-methyl, trifloxystrobin, and their base-mediated hydrolysis products.

kresoxim-methyl metabolite was previously observed as a rat excretion, found in both urine and fecal material, during toxicity experiments on rats.[26] The trifloxystrobin product has previously been found on crops such as wheat and beets.[27]

These results provide another example of where base-mediated hydrolysis of agrochemicals can occur at the conditions used during chemical softening with lime. We have previously reported on the based-mediated hydrolysis of thiamethoxam, a neonicotinoid insecticide,[13] and benoxacor, an herbicide safener.[17] Many water treatment plants in the agricultural Midwest of the U.S. rely on chemical softening using reagents like lime and soda ash due to the hardness of their source water. Notably, the products formed during the base-mediated hydrolysis of kresoxim-methyl and trifloxystrobin are more polar organic acids with ionizable groups. Because these transformation products are more hydrophilic than parent QoIs and have the potential to be anionic at certain pH values, it is likely they will exhibit different environmental fate profiles than the parent QoIs from which they are derived. Although the transformations observed *via* hydrolysis alter these QoIs at their known bioactive moieties (*i.e.*, their pharmacophore),[28] the extent to which these transformation products exhibit bioactivity as fungicides, or toward other non-target organisms, likely warrants further investigation.

QoI reaction with free chlorine

Five QoIs were found to be reactive toward free chlorine over relevant timescales such that at least partial transformation can be reasonably anticipated during water treatment and distribution. Fig. 2 shows concentration *versus* time profiles for the reaction of azoxystrobin, dimoxystrobin, kresoxim-methyl, pyraclostrobin and fenamidone with free chlorine at

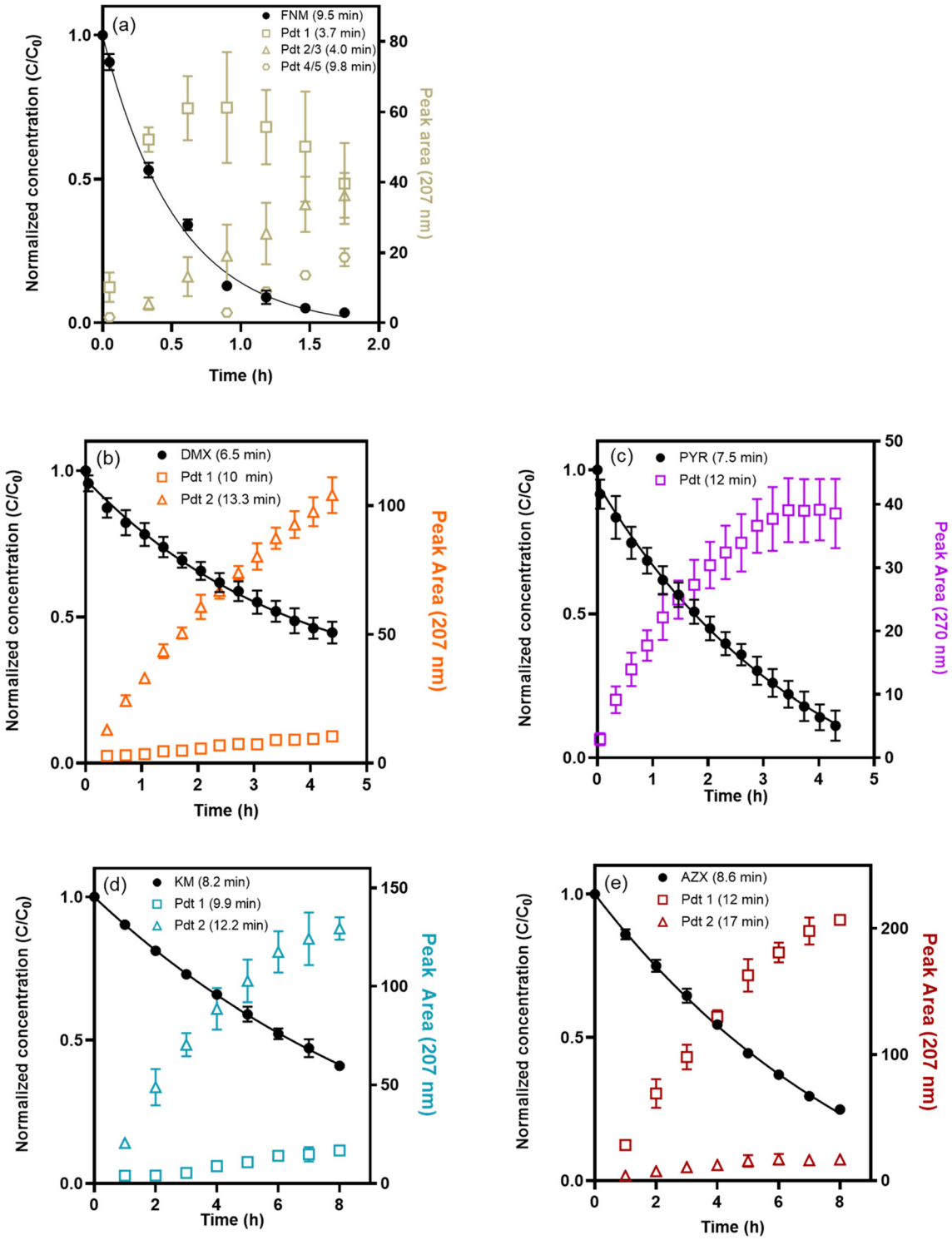

Fig. 2 Concentration *versus* time for QoIs (black, solid markers) and transformation products (colored, open markers) for the reaction of (a) 1 μM FNM + 5.6 mg L^{-1} HOCl as Cl_2, (b) 1 μM DMX + 7.7 mg L^{-1} HOCl as Cl_2, (c) 1.2 μM PYR + 5.6 mg L^{-1} HOCl as Cl_2, (d) 2 μM KM + 62 mg L^{-1} HOCl as Cl_2, and (e) 3 μM AZX + 62 mg L^{-1} HOCl as Cl_2. All reactions were conducted at pH 7 in 5–10 mM phosphate buffer.

pH 7. These five QoIs exhibited the greatest susceptibility to transformation in the presence of free chlorine under neutral pH conditions. In Fig. 2, concentration profiles are shown both for parent QoI decay and for the formation of product species detectable *via* HPLC-DAD over time based on absorbance at 207 nm (unless otherwise indicated).

At pH 7, reactions of azoxystrobin and kresoxim-methyl occurred over several hours and at higher concentrations of free chlorine (62 mg L^{-1} as Cl_2) relative to other QoIs, whereas dimoxystrobin, pyraclostrobin, and fenamidone reacted over shorter timescales under lower concentrations of free chlorine (5.6–7.7 mg L^{-1} as Cl_2). In all cases, QoI transformation at pH 7 followed exponential decay, consistent with a pseudo-first-order process under these experimental conditions (values of experimental k_{obs} are provided in Table S5).

From its acid dissociation constant (K_a value or $10^{-7.53}$),[17] HOCl remains the dominant chlorine species present at pH 7, representing ~75% of the total free chlorine. Assuming that HOCl is the active oxidant in our experimental systems and that the HOCl concentration ([HOCl]; present in at least a 10-fold excess in our systems) is reasonably constant over the duration of the reaction, we can use experimentally determined k_{obs} values from Table S5 to estimate second-order rate constants (k_{HOCl} values) for the reaction of each QoI with HOCl using eqn (1):

$$k_{HOCl} = k_{obs}/[HOCl] \quad (1)$$

Using this approach, we report k_{HOCl} values for azoxystrobin, dimoxystrobin, kresoxim-methyl, pyraclostrobin, and fenamidone in Table S6. The QoIs exhibit a wide range of reactivities toward HOCl; based on k_{HOCl} values, the most reactive species is fenamidone, which is roughly 200-fold more reactive than least-reactive kresoxim-methyl (k_{HOCl} values of 8.4 (±0.2) and 4.1 (±0.7) × 10^{-2} M^{-1} s^{-1}, respectively).

These values of k_{HOCl} are useful in estimating the extent of QoI transformation under conditions representative of drinking water treatment. For example, during municipal drinking water disinfection, typical chlorine doses can range from 1–10 mg Cl_2 L^{-1} and contact times within the distribution system (from chlorination to the first consumer) may vary from less than 1 hour up to 150 hours.[29] Chlorine residuals at the first consumer are typically ~1 mg Cl_2 L^{-1} but can range as high as 2 mg Cl_2 L^{-1} in some systems.[29]

Based upon these conditions, we can calculate half-lives of the QoIs, assuming a constant free chlorine concentration of 2 mg L^{-1} (as HOCl). Doing so results in half-lives of 0.79, 5.2, and 6.4 h for fenamidone, pyraclostrobin, and dimoxystrobin, respectively. Therefore, we would anticipate significant, if not complete, transformation of these QoIs during water treatment and distribution. Using these same assumptions, we see that azoxystrobin and kresoxim-methyl have considerably longer half-lives (~130 and ~170 h, respectively), suggesting at most partial transformation during treatment and distribution. For azoxystrobin and kresoxim-methyl, therefore, it is possible that both parent species and transformation products generated during chlorination may be present in finished drinking water and, potentially, at consumer taps.

Finally, to account for variability in pH that can arise through differences in source water and treatment processes prior to chlorination, we also conducted reactions with pyraclostrobin at pH 6 and 8. Values of k_{obs} for pyraclostrobin, determined from linear regression analysis of plots of the natural log of pyraclostrobin concentration *versus* time (Fig. 3a), decreased with increasing pH, with nearly a 10-fold drop from pH 6 [k_{obs} = 1.8 (±0.2) × 10^{-4} s^{-1}] to pH 8 [k_{obs} = 2.0 (±0.2) × 10^{-5} s^{-1}] (Table S7). This decrease in k_{obs} values is far greater than expected based on the corresponding change in HOCl concentration over the same pH range *via* dissociation to hypochlorite (ClO^-). From the K_a value of HOCl, its concentration should decrease from 97% of total free chlorine at pH 6 to 25% of total free chlorine at pH 8. Nevertheless, continuing with our assumption that HOCl is the active oxidant in these experimental systems, we find that k_{HOCl} values vary from 1.0 (±0.1) M^{-1} s^{-1} to 2.4 (±0.05) M^{-1} s^{-1} across the pH range investigated.

This variability in k_{HOCl} values suggests that our assumption of HOCl as the primary reactive species is likely invalid across the pH range considered. In fact, we observed a non-linear decrease in log(k_{obs}) values as a function of pH (Fig. 3b), as well as a non-first order relationship between log(k_{obs}) and log([HOCl]) values (inset, Fig. 3b), both of which suggest that other oxidants likely contribute to pyraclostrobin transformation. We hypothesize that low abundance yet highly reactive chlorine species such as chlorine monoxide (Cl_2O) and molecular chlorine (Cl_2), which have been demonstrated as important reactive entities toward other agrochemicals,[17,30] play an important role in the transformation of certain QoIs. Additional study is needed to examine the contribution of these minor chlorine species to QoI transformation under water treatment conditions. Although such work is beyond the scope of the current study, it is the focus of ongoing work in our laboratory.

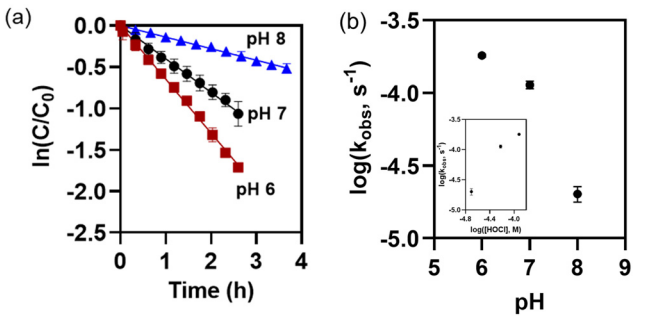

Fig. 3 (a) Natural log of normalized pyraclostrobin concentration (C/C_0) *versus* time, the slopes of which were used to determine k_{obs} values, and (b) log(k_{obs}) as a function of pH for the reaction of pyraclostrobin (initial concentration of 1.2 μM) with 5.6 mg L^{-1} HOCl as Cl_2 at pH 6, 7, and 8. Error bars indicate the standard deviation in log(k_{obs}) values for n = 3 measurements. Also in (b) we provide an inset showing the non-linear relationship between log(k_{obs} in s^{-1}) *versus* log([HOCl] in M).

QoI chlorination product analysis

Using HPLC-DAD with a reverse-phase C_{18} column, reaction product formation during chlorination was monitored over time. All product species of azoxystrobin, dimoxystrobin, kresoxim-methyl, and pyraclostrobin, and two products of fenamidone eluted later than their respective parent QoI. This is consistent with products of chlorination exhibiting greater hydrophobicity, and, in turn, different fate profiles and bioaccumulation potentials. Three fenamidone products eluted earlier than fenamidone, implying greater polarity and environmental mobility for these product species.

Product species identified by LC-HRMS and NMR analysis are shown in Fig. 4, with analytical results used in structure elucidation shown in Fig. S10–S60 and Tables S8–S17 in the SI. Key analytical details are as follows:

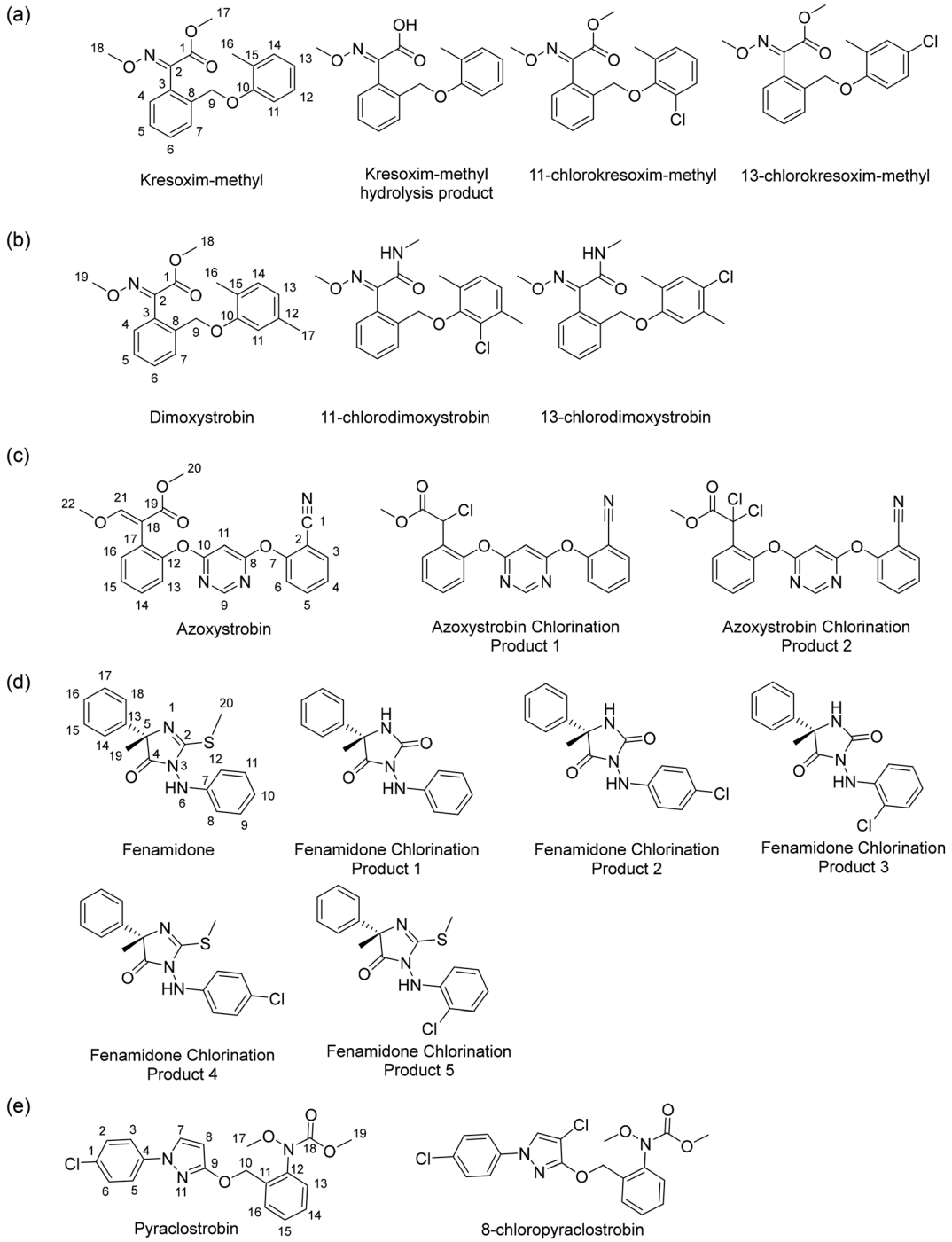

Fig. 4 Structures of parent QoIs and products generated during chlorination for (a) kresoxim-methyl, (b) dimoxystrobin, (c) azoxystrobin, (d) fenamidone, and (e) pyraclostrobin.

Kresoxim-methyl: We observed two major products from the chlorination of kresoxim-methyl. Based on HPLC-DAD detection at λ 207 nm, Product 1 (eluting at 9.9 min on the C_{18} column) was minor relative to Product 2 (eluting at 12.2 min) (see Fig. 2, with corresponding DAD trace from the scaled up reaction with separation *via* semi-preparative LC in Fig. S12).

11-Chlorokresoxim-methyl characterization

LC-HRMS analysis of kresoxim-methyl Product 1 gave an $[M + H]^+$ ion at *m*/*z* 348.0997 (Fig. S10), which established a molecular formula of $C_{18}H_{18}ClNO_4$ that corresponds to the loss of a hydrogen atom and the addition of a chlorine atom relative to the starting material. The ^{1}H NMR spectrum indicated the loss of a single proton signal in the aromatic region (Fig. S14), suggesting that an electrophilic aromatic chlorination reaction had occurred. ^{1}H NMR chemical shifts and coupling constants for protons at positions 4, 5, 6, and 7 remained similar to those of the starting material (Table S8). However, the three other signals in the aromatic region of the ^{1}H NMR spectrum (δ_H 7.18, d, 7.8 Hz; 6.96, t, 7.8 Hz; and 7.06, d, 7.8 Hz) are characteristic of a 1,2,3-trisubstituted pattern, and the δ-values are consistent with placement of the new chlorine atom at C-11. Placement at C-14 would also give a 1,2,3-pattern, but C-11 is activated toward electrophilic substitution by the presence of the oxygen atom substituent at C-10, while C-14 is not.[31] The δ-values are also more consistent with the structure shown due to the expected shift effects of the oxygen substituent.

13-Chlorokresoxim-methyl

LC-HRMS of kresoxim-methyl Product 2 gave an $[M + H]^+$ ion at *m*/*z* 348.0995 (Fig. S11), which established a molecular formula of $C_{18}H_{18}ClNO_4$, again corresponding to the loss of a hydrogen atom and the addition of a chlorine atom. The ^{1}H NMR spectrum indicated the loss of a single proton signal in the aromatic region (Fig. S15). The ^{1}H NMR chemical shifts and coupling constants for protons 4, 5, 6, and 7 remained similar to those of the starting material (Table S8). The three remaining aromatic signals (δ_H 6.64, d, 8.6 Hz; 7.02, dd, 2.8, 8.6 Hz; and 7.09, d, 2.8 Hz) were clearly consistent with a 1,2,4-trisubstituted pattern. Thus, it was determined that C-13 was the site of chlorination in this case. This is consistent with the electrophilic nature of the corresponding position in the ring. Chlorination at C-12 was considered unlikely, however, the NMR data further supported the proposed regiochemistry, as the upfield shift of the doublet showing only *ortho*-coupling (δ_H 6.64, d, 8.6 Hz) was consistent with it being the signal for H-11 due to the upfield shift effect of the C-10 oxygen substituent.[32]

Dimoxystrobin

We observed two major products for the chlorination of dimoxystrobin *via* HPLC-DAD detection at λ 207 nm, including a minor Product 1 that eluted earlier than major Product 2 (10 min and 13.3 min, respectively; see Fig. 2, with corresponding DAD trace from the scaled up reaction with separation *via* semi-preparative LC in Fig. S16).

11-Chlorodimoxystrobin characterization

LC-HRMS of dimoxystrobin Product 1 gave an $[M + H]^+$ ion at *m*/*z* 361.1310 (Fig. S18), which established a molecular formula of $C_{19}H_{21}ClN_2O_3$ that corresponds to the loss of a hydrogen atom and the addition of a chlorine atom relative to the dimoxystrobin starting material. The ^{1}H NMR spectrum indicated the loss of a single proton signal in the aromatic region (Fig. S21). ^{1}H NMR chemical shifts and coupling constants for protons 4, 5, 6, and 7 remained similar to those of the starting material (Table S9; Fig. S20 and S21). The two remaining aromatic signals (δ_H 6.96, d, 7.8 Hz; 6.91, d, 7.8 Hz) were *ortho*-coupled, leading to placement of the chlorine atom at C-11.

13-Chlorodimoxystrobin

LC-HRMS of dimoxystrobin Product 2 gave an $[M + H]^+$ ion at *m*/*z* 361.1310 (Fig. S19), which established a molecular formula of $C_{19}H_{21}ClN_2O_3$ that again corresponds to the loss of a hydrogen atom and the addition of a chlorine atom. The ^{1}H NMR spectrum again indicated the loss of a single proton signal in the aromatic region (Fig. S22). ^{1}H NMR chemical shifts and coupling constants for protons 4, 5, 6, and 7 remained similar to those of the starting material (Table S9). The two remaining aromatic signals (δ_H 6.63, s; 7.07, s) were both sharp singlets, leading to placement of the chlorine atom at C-13, because the two corresponding hydrogen atoms show no coupling to one another. All of the chlorination products obtained again had regiochemistry that was consistent with expectations for electrophilic aromatic substitution mechanisms.

Azoxystrobin

We observed two products of azoxystrobin chlorination, with Product 1 eluting earlier than Product 2 (12 and 17 min, respectively; see Fig. 2, with corresponding DAD trace from the scaled up reaction with separation *via* semi-preparative LC in Fig. S26). NMR assignments for Product 1 and Product 2 were made using a combination of 1D and 2D NMR techniques (Tables S10–S12; Fig. S28–S38). Analysis of Heteronuclear Single Quantum Coherence (HSQC) and Heteronuclear Multiple Bond Correlation (HMBC) data allowed for the assignment of all ^{13}C NMR shifts (Tables S11–S12; Fig. S31–S33). ^{1}H NMR assignments were determined by analysis of shifts, *J*-values, and COSY data (Table S10; Fig. S30).

Methyl-2(2-(6-(2-cyanophenoxy)-pyrimidin-4-yloxy)-phenyl)-2-chloroacetate

LC-HRMS data for azoxystrobin Product 1 showed an $[M + H]^+$ ion at *m*/*z* 396.0745 (Fig. S24) corresponding to the molecular formula $C_{20}H_{14}N_3O_4Cl$. The ^{1}H NMR spectrum (Fig. S34, Table

S10) indicated the loss of a methoxy group and the olefinic hydrogen relative to the starting material (Fig. S28, Table S10). Additionally, a new one-proton singlet appeared at δ 5.79. The presence of the new signal at δ 5.79, together with the loss of C_2H_3O relative to the starting material and the two signals noted above, could be rationalized through hydrolysis of the enol ether subunit of the β-methoxyacrylic ester moiety, followed by oxidation of the resulting aldehyde with subsequent decarboxylation,[33] and benzylic chlorination at the resulting newly formed methylene group. Chlorination at the benzylic α-carbon was consistent with the downfield shift of the corresponding benzylic proton singlet at δ 5.79. This product was sufficiently abundant to enable collection of ^{13}C NMR and HSQC data (Fig. S35–S37, Table S11) which were fully consistent with the assignment. These data included the presence of a new sp^3 methine carbon signal at δ_C 54.9 corresponding to the CHCl unit and correlating with the ^{1}H NMR singlet at δ 5.79 by HSQC. Interestingly, gradual loss of the remaining methoxy ^{1}H NMR signal was observed during 2D NMR data collection. HRMS confirmed that the signal loss was the result of exchange with the methanol-d_4 NMR solvent.

Methyl-2(2-(6-(2-cyanophenoxy)-pyrimidin-4-yloxy)-phenyl)-2,2-dichloroacetate

The ^{1}H NMR spectrum of azoxystrobin Product 2 (Fig. S38, Table S10) indicated the loss of the same methoxy group and vinyl proton signals relative to the starting material (Fig. S28; Table S10), however, no new ^{1}H NMR signals were observed in this case. LC-HRMS data showed an $[M + H]^+$ ion at m/z 430.0355 (Fig. S25) corresponding to the molecular formula $C_{20}H_{13}N_3O_4Cl_2$, which was consistent with the replacement of a hydrogen in azoxystrobin chlorination product 1 with a second chlorine atom. The absence of the new benzylic proton singlet observed in the ^{1}H NMR spectrum of the major product, combined with the difference in the formula, indicated that this minor product resulted from a second benzylic chlorination of the major product described above at the same α-carbon site. Although the amount of this minor product obtained was insufficient for collection of quality ^{13}C NMR data, this further chlorination at the same site was supported by additional downfield shifts of the signals for the nearby aromatic protons relative to those of the major product, especially that of the *ortho* proton signal for H-16.[34]

Fenamidone

We observed one major product for fenamidone using HPLC-DAD detection at λ 207 nm, though there was evidence for additional products that were gradually forming over longer timescales (see Fig. 2 and corresponding DAD trace from the scaled-up reaction with separation *via* semi-preparative LC in Fig. S39). This compound (Product 1) eluted earlier than the fenamidone parent (3.7 and 9.5 min, respectively) and was the primary and major product species. Product 1 did not continue to accumulate but rather decayed over time, suggesting it is likely reactive toward chlorine and subsequently degraded after formation. HRMS data for Product 1 showed an $[M + H]^+$ ion of m/z 282.1111, corresponding to a molecular formula of $C_{16}H_{15}N_3O_2$ (Fig. S43), indicating loss of CH_2S and addition of an oxygen atom relative to the starting material. The reaction was scaled up to enable collection of a sample of this product by semi-preparative HPLC for further analysis.

(*S*)-5-Methyl-5-phenyl-3-(phenylamino)-2,4-imidazolidine-dione

The ^{1}H NMR spectrum of fenamidone Product 1 (Fig. S49, Tables S14–S15) indicated the loss of a methyl group relative to the starting material (Fig. S47). Additionally, a new one-proton singlet appeared at δ 5.87. The presence of this new signal, together with the loss of CH_2S and addition of an oxygen atom relative to the starting material, can be rationalized through oxidation of the thiol subunit of the imidazole moiety, followed by subsequent hydrolysis to form an imidazoline ring, giving the fenamidone Product 1 structure shown in Fig. 4. The new signal at δ 5.87 corresponds to the amide-type NH present in the product. This compound, (*S*)-5-methyl-5-phenyl-3-(phenylamino)-2,4-imidazolidine-dione, also known as RPA 410193, was previously identified as a metabolic product of fenamidone, and the structure was confirmed by comparison with a standard spectrum of RPA 410193 (Fig. S49–S51).[35]

(5*S*)-8-Chloro-3-anilino-5-methyl-5-phenylimidazolidine-2,4-dione and (5*S*)-10-chloro-3-anilino-5-methyl-5-phenylimidazolidine-2,4-dione (Products 2 and 3)

Upon scaling up the reaction to enable isolation of fenamidone Product 1, four additional minor products were encountered in amounts that enabled their identification. Peaks for an additional pair of products eluting soon after Product 1 (Fig. S39) were only partially resolved. The corresponding peaks each gave an $[M + H]^+$ ion at m/z 316.0845 by LC-HRMS with a chlorine isotope peak at m/z 318.0816 corresponding to a molecular formula of $C_{16}H_{14}N_3O_2Cl$ (Fig. S44). This corresponds to addition of a chlorine atom and loss of a hydrogen atom relative to fenamidone Product 1. Although two HPLC peaks were present, they were collected together by semi-preparative HPLC because they did not fully separate (Fig. S39). The ^{1}H NMR spectrum of the resulting sample suggested a 3 : 1 mixture of products in the sample, which was consistent with the relative ratios of the two peaks in the HPLC-DAD chromatogram. However, it was possible to evaluate the two sets of NMR signals independently. The data for the major component (Product 2; Fig. S52, Table S14) confirmed the loss of a methyl unit and addition of a one-proton exchangeable proton signal corresponding to hydrolysis/oxygenation at C-2 and the associated amide NH as in Product 1. The ^{1}H NMR chemical shifts and coupling constants for protons 14–18 remained nearly the same as those of the starting material. However, the only two remaining proton signals of the major product in the sample (δ_H 6.68, distorted d, 8.8 Hz; 7.18,

distorted d, 8.8 Hz; 2H each) were clearly characteristic of a *para*-disubstituted benzene ring pattern, leading to the placement of the added chlorine atom at C-10.

The minor component of the sample (Product 3) contained signals matching those of Product 2 except that the *p*-disubstituted pattern was replaced by four one-proton signals (δ_H 6.54, dd, 7.8, 1.2 Hz; 6.88, td, 7.8, 1.4 Hz; 7.10, td, 7.8. 1.4; and 7.31, dd, 7.8, 1.2 Hz; Fig. S52, Table S14) consistent with a 1,2-disubstitution pattern, leading to the placement of the chlorine atom at C-8 in the corresponding product. The regiochemistry of substitution is consistent with expectations for electrophilic chlorination of Product 1.

8-Chlorofenamidone + 10-chlorofenamidone (Products 4 and 5)

Products 4 and 5 were significantly less abundant than Products 1–3, and co-eluted as a single peak after fenamidone in the semi-preparative HPLC chromatogram (Fig. S39). LC-HRMS data for this HPLC peak gave an $[M + H]^+$ ion at *m/z* 346.0770 corresponding to the molecular formula $C_{17}H_{16}N_3OSCl$ (Fig. S45). This mass corresponds to the loss of hydrogen and addition of a chlorine atom relative to fenamidone itself, which would be consistent with electrophilic substitution of the starting material by chlorine. Although the amount of material obtained was insufficient to afford quality NMR data, given this formula and the structures of Products 2 and 3 above, these products were presumed to be analogous, direct chlorination products of fenamidone with structures shown in Fig. 4.

The associated MS^2 fragmentation pattern (Fig. S46, Table S13) contains a peak at *m/z* 270.0789 corresponding to the molecular formula $C_{15}H_{13}N_3Cl$ and arising from a loss of 75.9981 (C_2H_4O). Additionally, there is a peak at *m/z* 126.0102 corresponding to the molecular formula $C_6H_5NCl^+$ arising from the loss of 220.0669 ($C_{11}H_{12}N_2OS$) supporting the expectation that chlorination had occurred on the aniline ring as shown in Fig. 4. Positioning of the Cl on C-8 and/or C-10 would be expected by analogy to Products 2 and 3, but this could not be determined on the basis of LC or MS data. Ultimately, it was judged likely that this peak consisted of both possible isomers (Products 4 and 5) by analogy to Products 2 and 3. Thus, Products 1, 4, and 5 are all formed from fenamidone *via* separate processes, and continue to react, giving rise to Products 2 and 3 as secondary products.

Pyraclostrobin

With HPLC-DAD detection at 207 nm, only one product was detected during the chlorination of pyraclostrobin (see Fig. 2, with corresponding DAD trace from the scaled up reaction with separation *via* semi-preparative LC in Fig. S53).

8-Chloropyraclostrobin

LC-HRMS gave an $[M + H]^+$ ion at *m/z* 422.0671 (Fig. S56), which established a molecular formula of $C_{19}H_{17}Cl_2N_3O_4$ that corresponds to the loss of a hydrogen atom and the addition of a chlorine atom. The ^1H NMR spectrum indicated the loss of single proton signal in the alkene region, corresponding to proton 8 (Fig. S58). ^1H NMR chemical shifts and coupling constants for protons 2–6, 10, 13–17 and 19 remained similar to those of the starting material (Fig. S57, Table S16). The remaining aromatic signal (δ_H 6.96, s) was a sharp singlet, compared to this signal being a one proton doublet in the starting material. This led to the addition of the Cl atom either at C-7 or C-8 on the pyrazole ring. To confirm placement of the Cl atom, a ^{13}C NMR spectrum was obtained for both the standard and chlorination product (Fig. S59 and S60, Table S17). The signal corresponding to C-8 shifted downfield in the spectrum compared with the starting material, while all other signals remained similar to the starting material. This information, combined with precedents for pyrazole chlorination reactions,[36,37] led to placement of the chlorine atom at C-8.

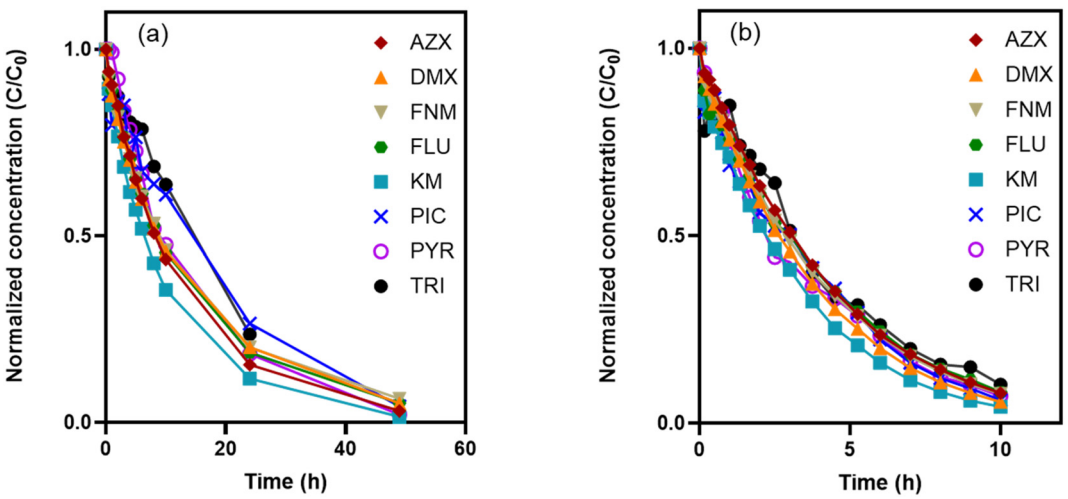

Fig. 5 Time-dependent QoI sorption data for (a) 0.5 g L^{-1} and (b) 1 g L^{-1} GAC in aqueous phosphate buffer (pH 7.5). QoIs were dosed at maximum solubility and rotated at 40 RPM.

QoI fate in activated carbon treatment systems

Fig. 5 shows the removal of various QoIs in well mixed batch systems with either 0.5 (Fig. 5a) or 1 g L^{-1} (Fig. 5b) of GAC. In both systems, we observed near complete uptake of QoIs, with the higher GAC loading producing shorter timescales for complete uptake (48 h for 0.5 g L^{-1} compared to 10 h for 1 g L^{-1}). Notably, there was little difference in the rate of uptake for the various QoIs, which may suggest that the rate of sorption is limited by mass transfer in our experimental systems (*e.g.*, QoI diffusion into the internal pores of GAC). We attribute the relatively fast and complete uptake of QoIs on GAC to their moderate to high hydrophobicity ($\log K_{ow}$ values ranging from 2.5 and 4.5 in Table S1), resulting in non-specific binding to the GAC surface and inside GAC pores *via* hydrophobic partitioning.

Conclusions and environmental implications

Herein, we demonstrate the inability of conventional water treatment operations to remove some QoI fungicides (*e.g.*, fluoxastrobin and picoxystrobin), whereas others are likely to be transformed during chemical softening and/or chlorination into reaction products with uncertain implications for human health effects through drinking water exposure. In areas where land use is dominated by agricultural activities, particularly conventional row cropping of corn and soybeans, evidence suggests that QoI fungicides are present in water resources, many of which serve as drinking water sources for the surrounding communities. Thus, their persistence and transformation through conventional treatment presents the opportunity for inadvertent exposure to QoIs and their transformation products through drinking water supplies. This exposure may prove hazardous to consumers in such areas because of recent evidence suggesting links between certain QoIs and neurodegenerative diseases.[38–40] We contend that this exposure threat is an issue of growing concern, especially as climate change and associated weather events increase soil moisture, thereby driving increases in fungicide use to prevent the growth of fungal pathogens on crops and ensure crop yields.[41] Moreover, fungicide wash-off into adjacent surface waters or underlying aquifers is also likely to increase with greater frequency of intense rainfall events, which is likely to result in higher detectable concentrations of QoIs in drinking water sources over time.[41]

For QoI transformation, we demonstrate that modulations in pH (for chemical softening) and redox conditions (for chemical disinfection) exploited for drinking water treatment can result in the reaction of certain QoI fungicides. In most instances documented in this work, the products that are generated *via* alkaline hydrolysis and chlorination are structurally analogous to parent QoIs. Notably, this work shows that QoIs with activated aromatic rings are generally susceptible to chlorination under chemical disinfection conditions to varying degrees. Only a modest level of activation was required, as three compounds containing benzene rings with a single oxygen or nitrogen substitution (dimoxystrobin, kresoxim-methyl, and fenamidone) were chlorinated to some extent *via* electrophilic aromatic substitution processes. Pyraclostrobin did not undergo such a reaction on its benzene units but instead was chlorinated on its central five-membered aromatic ring. Azoxystrobin, which contains a deactivating cyano substituent on one oxygenated benzene ring, underwent side-chain decomposition and benzylic halogenation elsewhere instead. This latter process was the most unusual and unexpected relative to the others observed. Neither trifloxystrobin nor picoxystrobin underwent detectable chlorination under these conditions, and both lack activating substituents on their benzene rings. As with all environmental transformation products identified through laboratory studies, there is need to validate the formation and occurrence of these species at the water treatment scale. This will require development of analytical standards and methods to facilitate such occurrence studies, as well as efforts to assess associated ecotoxicological risks posed by these transformation products.

Regarding the potential for retained bioactivity in the transformation products identified herein, the strobilurin pharmacophore is the β-methoxyacrylate-containing sidechain.[42,43] Within the β-methoxyacrylate moiety, it has been shown that only the carbonyl unit is required for biological activity.[42] On the other hand, hydrolysis of the methyl ester within the strobilurin pharmacophore has been shown to eliminate biological activity.[42,44] Increasing the lipophobicity of a compound through halogenation is an often used approach during drug development,[42] and our analysis suggests that the chlorinated products are more hydrophobic than their parent QoIs. Thus, products of QoI chlorination would be expected to exhibit environmental fate and bioaccumulation potentials distinct from those of the parent QoI species from which they are derived. Although toxicological evaluation of chlorination products is beyond the scope of the current study, it should be a priority going forward. In particular, unlike kresoxim-methyl and dimoxystrobin, azoxystrobin undergoes chlorination directly to its pharmacophore, and thus we contend that such testing should be prioritized for this compound in future work.

Finally, this work illustrates that activated carbon sorbents represent an effective management approach for QoI fungicides, as we have also found for other unregulated pesticide classes encountered in drinking water.[13] While an effective treatment option to remove QoIs from source waters, activated carbon is not a conventional treatment approach and thus is not widely used, particularly in smaller-scale water systems like those most typically encountered in the agricultural Midwest of the United States. Given our findings herein and in our prior work, there is growing need for smaller drinking water treatment plants that use source water that may contain agricultural runoff to implement

powdered or granular activated carbon treatment to improve water quality and minimize exposure to both regulated and emerging agrochemical classes.

Author contributions

CJK: methodology, validation, formal analysis, investigation, data curation, writing – original draft, writing – reviewing and editing, visualization. AMC: methodology, validation, formal analysis, investigation, data curation, writing – original draft, writing – reviewing and editing, visualization. SK: methodology, formal analysis, investigation, data curation, writing – original draft, visualization. JBG: conceptualization, methodology, formal analysis, resources, data curation, writing – review and editing, supervision. DMC: conceptualization, methodology, formal analysis, resources, data curation, writing – original draft, writing - review and editing, supervision, project administration, funding acquisition.

Conflicts of interest

There are no conflicts to declare.

Data availability

The data supporting this article have been included as part of the supplementary information (SI). Supplementary information includes detailed experimental methods, additional figures and tables associated with QoI fate during simulated water treatment, and all LC-MS/MS and NMR data used in product identification and structural elucidation. See DOI: https://doi.org/10.1039/d5ew01004g.

Acknowledgements

Funding for this project was provided by the Minnesota Environment and Natural Resources Trust Fund as recommended by the Legislative-Citizen Commission on Minnesota Resources (LCCMR). Support for AMC and SK was provided by the National Science Foundation Graduate Research Fellowship Program. Instrumentation used in product identification was funded in part by NSF Major Research Instrumentation grant CHE-1919422. Any opinions, findings, and conclusions or recommendations expressed in this material are those of the author(s) and do not necessarily reflect the views of the National Science Foundation. The authors would like to thank Profs. Kristine H. Wammer and Dalma Martinović-Weigelt from the University of St. Thomas for their thoughtful feedback and suggestions during the preparation of this work. The authors would also like to thank the two anonymous reviewers whose feedback improved the clarity of this work.

References

1 S. Savary, L. Willocquet, S. J. Pethybridge, P. Esker, N. McRoberts and A. Nelson, The Global Burden of Pathogens and Pests on Major Food Crops, *Nat. Ecol. Evol.*, 2019, **3**, 430–439.
2 S. Wegulo, J. Stevens, M. Zwingman and P. Stephen Baenziger, *Fungicides for Plant and Animal Diseases*, 2012, pp. 227–244.
3 F. Zeng, E. Arnao, G. Zhang, G. Olaya, J. Wullschleger, H. Sierotzki, R. Ming, B. H. Bluhm, J. P. Bond, A. M. Fakhoury and C. A. Bradley, Characterization of Quinone Outside Inhibitor Fungicide RSIstance in Cercospora Sojina and Development of Diagnostic Tools for Its Identification, *Plant Dis.*, 2015, **99**, 544–550.
4 C. C. Howell, K. T. Semple and G. D. Bending, Isolation and Characterisation of Azoxystrobin Degrading Bacteria From Soil, *Chemosphere*, 2014, **95**, 370–378.
5 V. Gandhi, R. Pankaj and C. Vishal Gandhi, New Generation Fungicides in Plant Disease Management, *Int. J. Chem. Stud.*, 2019, **7**, 3319–3323.
6 United States Geological Survey, *Pesticide National SynthSIs Project: Estimated Annual Agricultural Pesticide Use*.
7 University of Hertfordshire, *Pesticide Properties Database*.
8 K. L. Smalling, T. J. Reilly, M. W. Sandstrom and K. M. Kuivila, Occurrence and Persistence of Fungicides in Bed Sediments and Suspended Solids from Three Targeted Use Areas in the United States, *Sci. Total Environ.*, 2013, **447**, 179–185.
9 T. J. Reilly, K. L. Smalling, J. L. Orlando and K. M. Kuivila, Occurrence of Boscalid and Other Selected Fungicides in Surface Water and Groundwater in Three Targeted Use Areas in The United States, *Chemosphere*, 2012, **89**, 228–234.
10 N. Berenzen, A. Lentzen-Godding, M. Probst, H. Schulz, R. Schulz and M. Liess, A Comparison of Predicted and Measured Levels of Runoff-Related Pesticide Concentrations in Small Lowland Streams on a Landscape Level, *Chemosphere*, 2005, **58**, 683–691.
11 W. A. Battaglin, M. W. Sandstrom, K. M. Kuivila, D. W. Kolpin and M. T. Meyer, Occurrence of Azoxystrobin, Propiconazole, and Selected Other Fungicides in US Streams, 2005-2006, *Water, Air, Soil Pollut.*, 2011, **218**, 307–322.
12 Minnesota Department of Agriculture, *2021 Water Quality Monitoring Report*, 2022.
13 K. L. Klarich, N. C. Pflug, E. M. DeWald, M. L. Hladik, D. W. Kolpin, D. M. Cwiertny and G. H. LeFevre, Occurrence of Neonicotinoid Insecticides in Finished Drinking Water and Fate During Drinking Water Treatment, *Environ. Sci. Technol. Lett.*, 2017, **4**, 168–173.
14 J. Jiang, Y. Shi, R. Yu, L. Chen and X. Zhao, Biological Response of Zebrafish after Short-Term Exposure to Azoxystrobin, *Chemosphere*, 2018, **202**, 56–64.
15 S. Carey and J. K. Wolf, *Problem Formulation for the Ecological Risk and Drinking Water Exposure Assessments in Support of the Registration Review of Azoxystrobin*, Washington, 2009.
16 I. J. Tinsley, *Hydrolysis in Chemical Concepts in Pollutant Behavior*, John Wiley & Sons, 2004.
17 M. E. McFadden, E. V. Patterson, K. P. Reber, I. W. Gilbert, J. D. Sivey, G. H. LeFevre and D. M. Cwiertny, Acid- and Base-Mediated Hydrolysis of Dichloroacetamide Herbicide Safeners, *Environ. Sci. Technol.*, 2022, **56**, 325–334.

18 K. L. Klarich Wong, D. T. Webb, M. R. Nagorzanski, D. W. Kolpin, M. L. Hladik, D. M. Cwiertny and G. H. Lefevre, Chlorinated Byproducts of Neonicotinoids and Their Metabolites: An Unrecognized Human Exposure Potential?, *Environ. Sci. Technol. Lett.*, 2019, **6**, 98–105.

19 M. Deborde and U. von Gunten, Reactions of Chlorine with Inorganic and Organic Compounds During Water Treatment-Kinetics and Mechanisms: A Critical Review, *Water Res.*, 2008, 13–51.

20 J. Wei, Y. Chen, A. Tiemur, J. Wang and B. Wu, Degradation of Pesticide RSIdues by Gaseous Chlorine Dioxide on Table Grapes, *Postharvest Biol. Technol.*, 2018, **137**, 142–148.

21 R. P. Schwarzenbach, P. Gschwend and D. M. Imboden, *Environmental Organic Chemistry*, 2012.

22 M. L. Hladik, A. L. Roberts and E. J. Bouwer, Removal of Neutral Chloroacetamide Herbicide Degradates during Simulated Unit Processes for Drinking Water Treatment, *Water Res.*, 2005, **39**, 5033–5044.

23 M. A. Broadwater, T. L. Swanson and J. D. Sivey, Emerging Investigators Series: Comparing the Inherent Reactivity of Often-Overlooked Aqueous Chlorinating and Brominating Agents toward Salicylic Acid, *Environ. Sci.*, 2018, **4**, 369–384.

24 *Standard Methods for the Examination of Water and Wastewater*, ed. L. S. Clesceri, A. D. Eaton and A. E. Greenberg, American Public Health Association, 1998.

25 ENGIE, *2024 Consumer Confidence Report*, Iowa City, 2024.

26 *Pesticide RSIdues in Food-1998: Toxicology Evaluations: Joint Meeting of the FAO Panel of Experts on Pesticide RSIdues in Food and the Environment and the WHO Core Assessment Group, Rome, 21–30 September 1998, WHO/PCS/99.18*, World Health Organization, Geneva, 1999.

27 EFSA (European Food Safety Authority), M. Arena, D. Auteri, S. Barmaz, G. Bellisai, A. Brancato, D. Brocca, L. Bura, H. Byers, A. Chiusolo, D. Court Marques, F. Crivellente, C. De Lentdecker, M. De Maglie, M. Egsmose, Z. Erdos, G. Fait, L. Ferreira, M. Goumenou, L. Greco, A. Ippolito, F. Istace, J. Janossy, S. Jarrah, D. Kardassi, R. Leuschner, C. Lythgo, J. O. Magrans, P. Medina, I. Miron, T. Molnar, A. Nougadere, L. Padovani, J. M. Parra Morte, R. Pedersen, H. Reich, A. Sacchi, M. Santos, R. Serafimova, R. Sharp, A. Stanek, F. Streissl, J. Sturma, C. Szentes, J. Tarazona, A. Terron, A. Theobald, B. Vagenende, A. Verani and L. Villamar-Bouza, Conclusion on the peer review of the pesticide risk assessment of the active substance trifloxystrobin, *EFSA J.*, 2017, **15**(10), 4989.

28 A. Kunova, L. Palazzolo, F. Forlani, G. Catinella, L. Musso, P. Cortesi, I. Eberini, A. Pinto and S. Dallavalle, Structural Investigation and Molecular Modeling Studies of Strobilurin-Based Fungicides Active against the Rice Blast Pathogen *Pyricularia Oryzae*, *Int. J. Mol. Sci.*, 2021, **22**, 3731.

29 *Survey of Water Utility Disinfection Practices Water Quality Division Disinfection Committee*, 1992, vol. 84.

30 J. D. Sivey, C. E. McCullough and A. L. Roberts, Chlorine Monoxide (Cl2O) and Molecular Chlorine (Cl2) as Active Chlorinating Agents in Reaction of Dimethenamid with Aqueous Free Chlorine, *Environ. Sci. Technol.*, 2010, **44**, 3357–3362.

31 T. W. Graham Solomons, C. B. Fryhle and S. A. Snyder, *Organic Chemistry*, Wiley, 2016, pp. 661–710.

32 R. M. Silverstein, F. X. Webster, D. J. Kiemle and D. L. Bryce, *Spectrometric Identification of Organic Compounds*, Wiley, 2014.

33 A. Boudina, C. Emmelin, A. Baaliouamer, O. Païssé and J. M. Chovelon, Photochemical Transformation of Azoxystrobin in Aqueous Solutions, *Chemosphere*, 2007, **68**, 1280–1288.

34 E. Pretsch, P. Bühlmann and C. Affolter, *Tables of Spectral Data for Structure Determination of Organic Compounds*, Springer-Verlag Berlin and Heidelberg GmbH & Co. K, Berlin, 1989, p. H255.

35 R. López-Ruiz, R. Romero-González and A. Garrido Frenich, Dissipation Kinetics of Fenamidone, Propamocarb and Their Metabolites in Ambient Soil and Water Samples and Unknown Screening of Metabolites, *J. Environ. Manage.*, 2020, **254**, 109818.

36 K. L. Olsen, M. R. Jensen and J. A. MacKay, A Mild Halogenation of Pyrazoles Using Sodium Halide Salts and Oxone, *Tetrahedron Lett.*, 2017, **58**, 4111–4114.

37 B. V. Lyalin and V. A. Petrosyan, The Reactivity Trends in Electrochemical Chlorination and Bromination of N-Substituted and N-Unsubstituted Pyrazoles, *Chem. Heterocycl. Compd.*, 2014, **49**, 1599–1610.

38 J. Regueiro, N. Olguín, J. Simal-Gándara and C. Suñol, Toxicity Evaluation of New Agricultural Fungicides in Primary Cultured Cortical Neurons, *Environ. Res.*, 2015, **140**, 37–44.

39 K. Nguyen, C. L. Sanchez, E. Brammer-Robbins, C. Pena-Delgado, N. Kroyter, N. El Ahmadie, J. M. Watkins, J. J. Aristizabal-Henao, J. A. Bowden, C. L. Souders and C. J. Martyniuk, Neurotoxicity Assessment of QoI Strobilurin Fungicides Azoxystrobin and Trifloxystrobin in Human SH-SY5Y Neuroblastoma Cells: Insights from Lipidomics and Mitochondrial Bioenergetics, *Neurotoxicology*, 2022, **91**, 290–304.

40 J. Kang, K. Bishayee and S. O. Huh, Azoxystrobin Impairs Neuronal Migration and Induces ROS Dependent Apoptosis in Cortical Neurons, *Int. J. Mol. Sci.*, 2021, **22**, 12495.

41 I. Delcour, P. Spanoghe and M. Uyttendaele, Literature Review: Impact of Climate Change on Pesticide Use, *Food Res. Int.*, 2015, **68**, 7–15.

42 H. Sauter, W. Steglich and T. Anke, Strobilurins: Evolution of a New Class of Active Substances, *Angew. Chem., Int. Ed.*, 1999, **38**, 1328–1349.

43 M. Zuccolo, A. Kunova, L. Musso, F. Forlani, A. Pinto, G. Vistoli, S. Gervasoni, P. CortSI and S. Dallavalle, Dual-Active Antifungal Agents Containing Strobilurin and SDHI-Based Pharmacophores, *Sci. Rep.*, 2019, **9**, 11377.

44 H. Balba, Review of Strobilurin Fungicide Chemicals, *J. Environ. Sci. Health, Part B*, 2007, **42**, 441–451.